

# Graph Theoretical Analysis Reveals: Women’s Brains are Better Connected than Men’s

Balázs Szalkai<sup>a</sup>, Bálint Varga<sup>a</sup>, Vince Grolmusz<sup>a,b,\*</sup>

<sup>a</sup>*PIT Bioinformatics Group, Eötvös University, H-1117 Budapest, Hungary*

<sup>b</sup>*Uratim Ltd., H-1118 Budapest, Hungary*

---

## Abstract

Deep graph-theoretic ideas in the context with the graph of the World Wide Web led to the definition of Google’s PageRank and the subsequent rise of the most-popular search engine to date. Brain graphs, or connectomes, are being widely explored today. We believe that non-trivial graph theoretic concepts, similarly as it happened in the case of the World Wide web, will lead to discoveries enlightening the structural and also the functional details of the animal and human brains. When scientists examine large networks of tens or hundreds of millions of vertices, only fast algorithms can be applied because of the size constraints. In the case of diffusion MRI-based structural human brain imaging, the effective vertex number of the connectomes, or brain graphs derived from the data is on the scale of several hundred today. That size facilitates applying strict mathematical graph algorithms even for some hard-to-compute (or NP-hard) quantities like vertex cover or balanced minimum cut.

In the present work we have examined brain graphs, computed from the data of the Human Connectome Project, recorded from male and female subjects between ages 22 and 35. Significant differences were found between the male and female structural brain graphs: we show that the average female connectome has more edges, is a better expander graph, has larger minimal bisection width, and has more spanning trees than the average male connectome. Since the average female brain weights less than the brain of males, these properties show that the female brain is more “well-connected” or perhaps, more “efficient” in a sense than the brain of males. It is known that the female brain has a larger white matter/gray matter ratio than the brain of males; this observation is in line with our findings concerning the number of edges, since the white matter consists of myelinated axons, which, in turn, correspond to the connections in the brain graph. We have also found that the minimum bisection width, normalized with the edge number, is also significantly larger in the right and the left hemispheres in females: therefore, that structural difference is independent from the difference in the number of edges.

---

\*Corresponding author

*Email addresses:* [szalkai@pitgroup.org](mailto:szalkai@pitgroup.org) (Balázs Szalkai), [varga@pitgroup.org](mailto:varga@pitgroup.org) (Bálint Varga), [grolmusz@pitgroup.org](mailto:grolmusz@pitgroup.org) (Vince Grolmusz)

---

## 1. Introduction

In the last several years hundreds of publications appeared describing or analyzing structural or functional networks of the brain, frequently referred to as "connectome" [1, 2]. Some of these publications analyzed data from healthy humans [3, 4, 5, 6], and some compared the connectome of the healthy brain with diseased one [7, 8, 9, 10, 11].

So far, the analyses of the connectomes mostly used tools developed for very large networks, such as the graph of the World Wide Web (with billions of vertices), or protein-protein interaction networks (with tens or hundreds of thousands of vertices), and because of the huge size of original networks, these methods used only very fast algorithms and frequently just primary degree statistics and graph-edge counting between pre-defined regions or lobes of the brain [12].

In the present work we demonstrate that deep and more intricate graph theoretic parameters could also be computed by using, among other tools, contemporary integer programming approaches for connectomes with several hundred vertices.

With these mathematical tools we show statistically significant differences in some graph properties of the connectomes, computed from MRI imaging data of male and female brains. We will not try to associate behavioral patterns of males and females with the discovered structural differences [12] (see also the debate that article has generated: [13, 14, 15]), because we do not have behavioral data of the subjects of the imaging study, and, additionally, we cannot describe high-level functional properties implied by those structural differences. However, we clearly demonstrate that deep graph-theoretic parameters show "better" connections in a certain sense in female connectomes than in male ones.

The study of [12] analyzed the 95-vertex graphs of 949 subjects aged between 8 and 22 years, using basic statistics for the numbers of edges running either between or within different lobes of the brain (the parameters deduced were called *hemispheric connectivity ratio*, *modularity*, *transitivity* and *participation coefficients*, see [12] for the definitions). It was found that males have significantly more intra-hemispheric edges than females, while females have significantly more inter-hemispheric edges than males.

## 2. Results and Discussion

We have analyzed the connectomes of 96 subjects, 52 females and 44 males, each with 83, 129 and 234 node resolutions, and each graphs with five different weight functions. We considered the connectomes as graphs with weighted edges, and performed graph-theoretic analyses with computing some polynomial-time computable and also some NP-hard graph parameters on the individual graphs, and then compared the results statistically for the male and the female group.

We have found that female connectomes have more edges, larger (normalized) minimum bisection widths, larger minimum-vertex covers and more spanning trees than the male connectomes.

In order to describe the parameters, which differ significantly among male and female connectomes, we need to place them in the context of their graph theoretical definitions.

### 2.1. Edge number and edge weights

We have found significantly higher number of edges (counted with 5 types of weights and also without any weights) in both hemispheres and also in the whole brain in females, in all resolutions. This finding is surprising, since we used the same parcellation and the same tractography and the same graph-construction methods for female and male brains, and because it is proven that females have, on average, less-weighting brains than males [16]. For example, in the 234-vertex resolution, the average number of (unweighted) edges in female connectomes is 1826, in males 1742, with  $p = 0.00063$  (see the Appendix for tables with the results). The work of [12] reported similar findings in inter-hemispheric connections only.

It is known that there are statistical differences in the size and the weight of the female and the male cerebra [16]. It was also published [17] that female brains statistically have a higher white matter/gray matter ratio than male brains. We argue that this observation is in line with the quantitative differences in the fibers and edges in the connectomes of the sexes.

In a simplified view, the edges of the braingraph correspond to the fibers of the myelinated axons in the white matter, while the nodes of the graph to areas of the gray matter. Therefore, since females have a higher white matter/gray matter ratio than males by [17] that fact implies that the number of detected fibers by the tractography step of the processing is relatively higher in females than in males, and this higher number of fibers imply higher number of edges in female connectomes.

### 2.2. Minimum cut and balanced minimum cut

Suppose the nodes, or the vertices, of a graph are partitioned into two, disjoint, non-empty sets, say  $X$  and  $Y$ ; their union is the whole vertex-set of the graph. The  $X, Y$  cut is the set of *all* edges connecting vertices of  $X$  with the vertices of  $Y$  (Figure 1A). The size of the cut is the number of edges in the cut. In graph theory, the size of the minimum cut is an interesting quantity. The minimum cut between vertices  $a$  and  $b$  is the minimum cut, taken for all  $X$  and  $Y$ , where vertex  $a$  is in  $X$  and  $b$  is in  $Y$ . This quantity gives the “bottleneck”, in a sense, between those two nodes (c.f., Menger theorems and Ford-Fulkerson’s Min-Cut-Max-Flow theorem [18, 19]). The minimum cut in a graph is defined to be the cut with the fewest edges for *all* non-empty sets  $X$  and  $Y$ , partitioning the vertices.

Clearly, for non-negative weights, the size of the minimum cut in a non-connected graph is 0. Very frequently, however, in connected graphs, the minimum cut is determined by just the smallest degree node: that node is the only

element of set  $X$  and all the other vertices of the graph are in  $Y$  (Figure 1B). Because of this phenomenon, the minimum cut is frequently queried for the “balanced” case, when the size (i.e., the number of vertices) of  $X$  and  $Y$  needs to be equal (or, more exactly, may differ by at most one if the number of the vertices of the graph is odd), see Figure 1C. This problem is referred to as *the balanced minimum cut* or the *minimum bisection* problem. If the minimum bisection is small that means that there exist a partition of the vertices into two sets of equal size that are connected with only a few edges. If the minimum bisection is large then the two half-sets in *every possible bisections* of the graph are connected by many edges.

Therefore, the balanced minimum cut of a graph is independent of the particular labeling of the nodes. The number of all the balanced cuts in a graph with  $n$  vertices is greater than

$$\frac{1}{n+1}2^n,$$

that is, for  $n = 250$ , this number is very close to the number of atoms in the visible universe [20]. Consequently, one cannot practically compute the minimum bisection width by reviewing all the bisections in a graph of that size. Moreover, the complexity of computing this quantity is known to be NP-hard [21] in general, but with contemporary integral programming approaches, for the graph-sizes we are dealing with, the exact values are computable.

In computer engineering, an important measure of the quality of an interconnection network is its minimum bisection width [22]: the higher the width is the better the network.

For the whole brain graph, as it is anticipated, we have found that the minimum balanced cut is almost exactly represents the edges crossing the *corpus callosum*, connecting the two cerebral hemispheres.

We show that within both hemispheres, the minimum bisection size of female connectomes are significantly larger than the minimum bisection size of the males. Much more importantly, we show that this remains true if we *normalize with the sum of all edge-weights*: that is, *this phenomenon cannot be due* to the higher number of edges or the greater edge weights in the female brain: it is an intrinsic property of the female brain graph in our data analyzed.

For example, in the 234-vertex resolution, in the left hemisphere, the normalized balanced minimum cut in females, on the average, is 0.09416, in the males 0.07896,  $p = 0.00153$  (see the Appendix for tables with the results).

We think that this finding is one of the main results of the present work: even if the significant difference in the weighted edge numbers are due to some artifacts in the data acquisition/processing workflow, the normalized balanced minimum cut size seems to be independent from those processes.

### 2.3. Eigengap and the expander property

Expander graphs and the expander-property of graphs are one of the most interesting area of graph theory: they are closely related to the convergence rate and the ergodicity of Markov chains, and have applications in the design

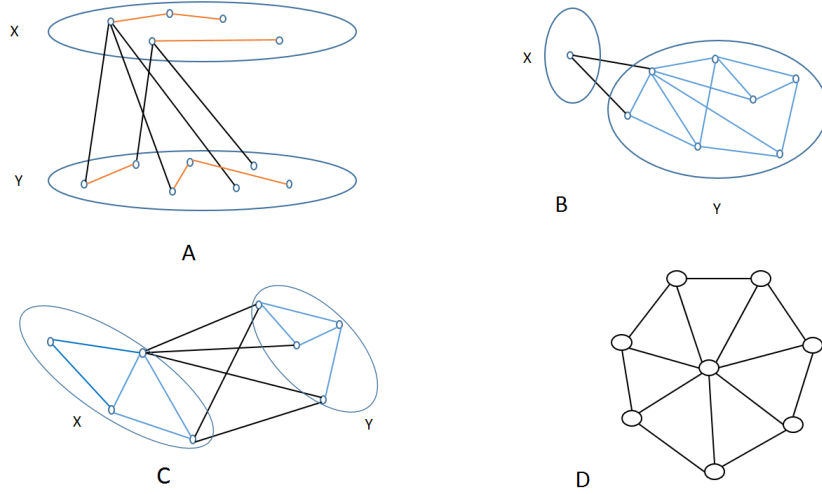


Figure 1: Panel A: An X-Y cut. The cut-edges are colored black. Panel B: An un-balanced minimum cut. Panel C: A balanced cut. Panel D: The wheel graph.

of communication- and sorting networks and methods for de-randomizing algorithms [23]. A graph is an  $\epsilon$ -expander, if every – not too small and not too large – vertex-set  $S$  of the graph has at least  $\epsilon|S|$  outgoing edges (see [23] for the exact definition).

Random walks on good expander graphs converge very fast to the limit distribution: this means that good expander graphs, in a certain sense, are “intrinsically better” connected than bad expanders. It is known that large eigengap of the walk transition matrix of the graph implies good expansion property [23].

We have found that women’s connectomes have significantly larger eigengap, and, consequently, they are better expander graphs than the connectomes of men. For example, in the 83-node resolution, in the left hemisphere and in the unweighted graph, the average female connectome’s eigengap is 0.306 while in the case of men it is 0.272, with  $p = 0.00458$ .

#### 2.4. The number of spanning forests

A *tree* in graph theory is a connected, cycle-free graph. Any tree on  $n$  vertices has the same number of edges:  $n - 1$ . Trees, and tree-based structures are common in science: phylogenetic trees, hierarchical clusters, data-storage on hard-disks, or a computational model called *decision trees* all apply graph-theoretic trees. A *spanning tree* is a minimal subgraph of a connected graph that is still connected. Some graphs have no spanning trees at all: only connected

graphs have spanning trees. A tree has only one spanning tree: itself. Any connected graph on  $n$  vertices has a minimum of  $n - 1$  and a maximum of  $n(n - 1)/2$  edges [24]. A connected graph with few edges still may have exponentially many different spanning trees: e.g., the  $n$ -vertex wheel on Figure 1D has at least  $2^{n-1}$  spanning trees (for  $n \geq 4$ ). Cayley’s famous theorem, and its celebrated proof with Prüfer codes [25] shows that the number of spanning trees of the complete graph on  $n$  vertices is  $n^{n-2}$ .

If a graph is not connected, then it contains more than one connected components. Each connected component has at least one spanning tree, and the whole graph has at least one *spanning forest*, comprising of the spanning trees of the components. The number of spanning forests is clearly the product of the numbers of the spanning trees of the components.

For graphs in general, one can compute the number of their spanning forests by Kirchoff’s matrix tree theorem [26, 27] using the eigenvalues of the Laplacian matrix [27] of the graph.

We show that female connectomes have significantly higher number of spanning trees than the connectomes of males. For example, in the 129-vertex resolution, in the left hemisphere, the logarithm of the number of the spanning forests in the unweighted case are 162.01 in females, 158.88 in males with  $p = 0.013$ .

### 3. Materials and Methods

#### 3.1. Data source and graph computation:

The dataset applied is a subset of the Human Connectome Project [28] anonymized 500 Subjects Release: (<http://www.humanconnectome.org/documentation/S500>) of healthy subjects between 22 and 35 years of age. Data was downloaded in October, 2014. The Connectome Mapper Toolkit [29] (<http://cmtk.org>) was applied for brain tissue segmentation into grey and white matter, partitioning, tractography and the construction of the graphs from the fibers identified in the tractography step. The Connectome Mapper Toolkit [29] default partitioning was used (computed by the FreeSurfer, and based on the Desikan-Killiany anatomical atlas) into 83, 129 and 234 cortical and sub-cortical structures (as the brainstem and deep-grey nuclei), referred to as “Regions of Interest”, ROIs, (see Figure 4 in [29]). Tractography was performed by choosing the deterministic streamline method [29] with randomized seeding.

The graphs were constructed as follows: the nodes correspond to the ROIs in the specific resolution. Two nodes were connected by an edge if there exists at least one fiber (determined by the tractography step) connecting the ROIs, corresponding to the nodes. More than one fibers, connecting the same nodes, may give rise to the weight of that edge, depending on the weighting method. Loops were deleted from the graph.

The weights of the edges are assigned by several methods, taking into account the lengths and the multiplicities of the fibers, connecting the nodes:

- **Unweighted:** Each edge has weight 1.

- **FiberN**: The number of fibers traced along the edge: this number is larger than one if more than one fibers connect two cortical or sub-cortical areas, corresponding to the two endpoints of the edge.
- **FAMean**: The arithmetic mean of the fractional anisotropies [30] of the fibers, belonging to the edge.
- **FiberLengthMean**: The average length of the fibers, connecting the two endpoints of the edge.
- **FiberNDivLength**: The number of fibers belonging to the edge, divided by their average length. This quantity is related to the simple electrical model of the nerve fibers: by modeling the fibers as electrical resistors with resistances proportional to the average fiber length, this quantity is precisely the conductance between the two regions of interest. Additionally, **FiberNDivLength** can be observed as a reliability measure of the edge: longer fibers are less reliable than the shorter ones, due to possible error accumulation in the tractography algorithm that constructs the fibers from the anisotropy data. Multiple fibers connecting the same two ROIs, corresponding to the endpoints, add to the reliability of the edge, because of the independently tractographed connections.

By *generalized adjacency matrix* we mean a matrix of size  $n \times n$  where  $n$  is the number of *nodes* (or *vertices*) in the graph, whose rows and columns correspond to the nodes, and whose each element is either zero if there is no edge between the two nodes, or equals to the weight of the edge connecting the two nodes. By the *generalized degree* of a node we mean the sum of the weights of the edges adjacent to that node. Note that the generalized degree of the node  $v$  is exactly the sum of the elements in the row (or column) of the generalized adjacency matrix corresponding to  $v$ . By *generalized Laplacian matrix* we mean the matrix  $D - A$ , where  $D$  is a diagonal matrix containing the generalized degrees, and  $A$  is the generalized adjacency matrix.

### 3.2. Graph parameters:

We calculated various graph parameters for each brain graph and weight function. These parameters included:

- **Number of edges (Sum)**. The weighted version of this quantity is the sum of the weights of the edges.
- **Normalized largest eigenvalue (AdjLMaxDivD)**: The largest eigenvalue of the generalized adjacency matrix, divided by the average degree. Dividing by the average degree of vertices was necessary because the largest eigenvalue is bounded by the average- and maximum degrees, and thus is considered by some a kind of “average degree” itself [24]. This means that a denser graph may have a bigger  $\lambda_{max}$  largest eigenvalue solely because of a larger average degree. We note that the average degree is already defined by the sum of weights.

- Eigengap of the transition matrix (**PGEigengap**): The transition matrix  $P_G$  is obtained by dividing all the rows of the generalized adjacency matrix by the generalized degree of the corresponding node. When performing a random walk on the graph, for nodes  $i$  and  $j$ , the corresponding matrix element describes the probability of transitioning to node  $j$ , supposing that we are at node  $i$ . The eigengap of a matrix is the difference of the largest and the second largest eigenvalue. It is characteristic to the expander properties of the graph: the larger the gap, the better expander is the graph (see [23] for the exact statements and proofs).
- Hoffman’s bound (**HoffmanBound**): The expression

$$1 + \frac{\lambda_{max}}{|\lambda_{min}|},$$

where  $\lambda_{max}$  and  $\lambda_{min}$  denote the largest and smallest eigenvalues of the adjacency matrix. It is a lower bound for the chromatic number of the graph. The chromatic number is generally higher for denser graphs, as the addition of an edge may make a previously valid coloring invalid.

- Logarithm of number of spanning forests (**LogAbsSpanningForestN**): The number of the spanning trees in a connected graph can be calculated from the spectrum of its Laplacian [26, 27]. Denser graphs tend to have more spanning trees, as the addition of an edge introduces zero or more new spanning trees. If a graph is not connected, then the number of spanning forests is the product of the numbers of the spanning trees of the components. The parameter **LogAbsSpanningForestN** equals to the logarithm of the number of spanning forests in the unweighted case. In the case of other weight functions, if we define the weight of a tree by the product of the weights of its edges, then this parameter equals to the sum of the logarithms of the weights of the spanning trees in the forests.
- Balanced minimum cut, divided by the number of edges (**MinCutBalDivSum**): The task is to partition the graph into two sets whose size may differ from each other by at most 1, so that the number of edges crossing the cut is minimal. This is the “balanced minimum cut” problem, or sometimes called the “minimum bisection width” problem. For the whole brain graph, our expectation was that the minimum cut corresponds to the boundary of the two hemispheres, which was indeed proven when we analyzed the results.
- Minimum cost spanning tree (**MinSpanningForest**), calculated with Kruskal’s algorithm.
- Minimum weighted vertex cover (**MinVertexCover**): Each vertex should have a (possibly fractional) weight assigned such that, for each edge, the sum of the weights of its two endpoints is at least 1. This is the fractional relaxation of the NP-hard vertex-cover problem [31]. The minimum of the sum of all vertex-weights is computable by a linear programming approach.



- Minimum vertex cover (**MinVertexCoverBinary**): Same as above, but each weight must be 0 or 1. In other words, a minimum size set of vertices is selected such that each edge is covered by at least one of the selected vertices. This NP-hard graph-parameter is computed only for the unweighted case. The exact values are computed by an integer programming solver SCIP (<http://scip.zib.de>), [32, 33].

The above 9 parameters were computed for all three resolutions and for the left and the right hemispheres and also for the whole connectome, with all 5 weight functions (with the following exceptions: **MinVertexCoverBinary** was computed only for the unweighted case, and the **MinSpanningForest** was not computed for the unweighted case).

### 3.3. Statistical analysis

Since each connectome was computed in multiple resolutions (in 83, 129 and 234 nodes), we had three graphs for each brain. In addition, the parameters were calculated separately for the connectome within the left and right hemispheres as well, not only the whole graph, since we intended to examine whether statistically significant differences can be attributed to the left or right hemispheres. Each subjects' brain was corresponded to 9 graphs (3 resolutions, each in the left and the right hemispheres, plus the whole cortex with sub-cortical areas) and for each graph we calculated 9 parameters, each (with the exceptions noted above) with 5 different edge weights. This means that we assigned  $7 \cdot 5 \cdot 3 + 1 \cdot 3 + 4 \cdot 3 = 120$  attributes to each resolution of the 96 brains, that is, 360 attributes to each brain.

The statistical null hypothesis [34] of ours was that the graph parameters do not differ between the male and the female groups. As the first approach, we have used ANOVA (Analysis of variance) [35] to assign p-values for all parameters in each hemispheres and in each resolutions and in each weight-assignments.

Our very large number of attributes may lead to false negatives, i.e., to “type II” statistical errors: in other words, it may happen that an attribute, with a very small p-value may appear “at random”, simply because we tested a lot of attributes. In order to deal with “type II” statistical errors, we followed the route described below.

We divided the population randomly into two sets by the parity of the sum of the digits in their ID. The first set was used for making hypotheses and the second set for testing these hypotheses. This was necessary to avoid type II errors resulting from multiple testing correction. If we made hypotheses for all the numerical parameters, then the Holm-Bonferroni correction [36] we used would have unnecessarily increased the p-values. Thus we needed to filter the hypotheses first, and that is why we needed the first set. Testing on the first set allowed us to reduce the number of hypotheses and test only a few of them on the second set.

The hypotheses were filtered by performing ANOVA (Analysis of variance) [35] on the first set. Only those hypotheses were selected to qualify for the second round where the p-value was less than 1%. The selected hypotheses

were then tested for the second set as well, and the resulting p-value corrected with the Holm-Bonferroni correction method [36] with a significance level of 5%.

In Table 1 those hypotheses rejected were highlighted in bold, meaning that *all* the corresponding graph parameters differ significantly in sex groups at a combined significance level of 5%.

We also highlighted (in italic) those p-values which were individually less than the threshold, meaning that these hypotheses can *individually* be rejected at a level of 5%, but it is very likely that *not all* of these graph parameters are significantly different between the sexes.

#### 4. Conclusions:

We have computed 83-, 129- and 234-vertex-graphs from the diffusion MRI images of the 96 subjects of 52 females and 44 males, between the age of 22 and 35. We have found, after a careful statistical analysis, significant differences between some graph theoretical parameters of the male and female brain graphs. Our findings show that the female brain graphs have generally more edges (counted with and without weights), have larger normalized minimum bisection widths and have more spanning trees (counted with and without weights) than the connectomes of males (Table 1). Additionally, with weaker statistical validity, some spectral properties and the minimum vertex cover also differ in the connectomes of different sexes (each with  $p < 0.02$ ).

#### 5. Data availability:

The unprocessed and pre-processed MRI data is available at the Human Connectome Project’s website:

<http://www.humanconnectome.org/documentation/S500> [28].

##### 5.1. Table 1

Scale	Property	p (1st)	p (2nd)	p (corrected)
129	Right_MinCutBalDivSum_FAMean	0.00807	<i>0.00003</i>	<b>0.00401</b>
83	All_LogSpanningForestN_FiberNDivLength	0.00003	<i>0.00004</i>	<b>0.00451</b>
234	All_PGEigengap_FiberNDivLength	0.00321	<i>0.00007</i>	<b>0.00798</b>
129	All_PGEigengap_FiberNDivLength	0.00792	<i>0.00011</i>	<b>0.01303</b>
83	Left_MinCutBalDivSum_FiberN	0.00403	<i>0.00011</i>	<b>0.01300</b>
83	Right_MinCutBalDivSum_FAMean	0.00496	<i>0.00015</i>	<b>0.01744</b>
129	Left_PGEigengap_FiberNDivLength	0.00223	<i>0.00015</i>	<b>0.01797</b>
234	All_PGEigengap_FiberN	0.00826	<i>0.00022</i>	<b>0.02517</b>
83	All_Sum_Unweighted	0.00025	<i>0.00022</i>	<b>0.02504</b>
129	Left_MinCutBalDivSum_FiberN	0.00001	<i>0.00023</i>	<b>0.02563</b>
83	All_LogSpanningForestN_FiberN	0.00001	<i>0.00028</i>	<b>0.03084</b>
83	Right_Sum_FAMean	0.00028	<i>0.00029</i>	<b>0.03224</b>
234	All_Sum_Unweighted	0.00063	<i>0.00032</i>	<b>0.03512</b>
234	Left_PGEigengap_FiberNDivLength	0.00013	<i>0.00038</i>	<b>0.04171</b>
129	All_Sum_Unweighted	0.00026	<i>0.00042</i>	<b>0.04563</b>

234	All_Sum_FAMean	0.00014	<i>0.00047</i>	<b>0.04988</b>
129	All_LogSpanningForestN_FiberN	0.00000	<i>0.00048</i>	0.05045
83	All_Sum_FAMean	0.00029	<i>0.00050</i>	0.05260
129	Right_Sum_FAMean	0.00062	<i>0.00051</i>	0.05355
234	Right_PGEigengap_FiberNDivLength	0.00041	<i>0.00053</i>	0.05414
83	Left_Sum_Unweighted	0.00378	<i>0.00068</i>	0.06936
234	Right_Sum_FAMean	0.00085	<i>0.00084</i>	0.08454
234	Left_Sum_Unweighted	0.00293	<i>0.00092</i>	0.09212
129	All_Sum_FAMean	0.00015	<i>0.00097</i>	0.09650
234	Left_MinCutBalDivSum_FiberN	0.00002	<i>0.00108</i>	0.10539
83	Left_LogSpanningForestN_FiberNDivLength	0.00343	<i>0.00116</i>	0.11274
83	All_LogSpanningForestN_Unweighted	0.00113	<i>0.00121</i>	0.11629
234	Left_MinCutBalDivSum_FiberLengthMean	0.00411	<i>0.00123</i>	0.11646
83	All_LogSpanningForestN_FAMean	0.00012	<i>0.00126</i>	0.11823
83	Right_Sum_Unweighted	0.00019	<i>0.00128</i>	0.11891
129	Left_MinCutBalDivSum_Unweighted	0.00265	<i>0.00134</i>	0.12351
83	Left_MinCutBalDivSum_Unweighted	0.00206	<i>0.00136</i>	0.12370
129	Left_PGEigengap_FiberN	0.00382	<i>0.00142</i>	0.12775
234	All_LogSpanningForestN_FAMean	0.00043	<i>0.00150</i>	0.13343
234	Left_PGEigengap_FiberN	0.00066	<i>0.00163</i>	0.14369
129	Right_LogSpanningForestN_FAMean	0.00143	<i>0.00170</i>	0.14769
83	Left_MinCutBalDivSum_FiberNDivLength	0.00031	<i>0.00175</i>	0.15023
129	All_LogSpanningForestN_FiberNDivLength	0.00000	<i>0.00177</i>	0.15009
129	All_LogSpanningForestN_Unweighted	0.00218	<i>0.00182</i>	0.15279
129	Right_Sum_Unweighted	0.00068	<i>0.00186</i>	0.15417
129	Left_PGEigengap_FAMean	0.00995	<i>0.00191</i>	0.15694
129	All_LogSpanningForestN_FAMean	0.00019	<i>0.00211</i>	0.17093
234	Left_Sum_FAMean	0.00026	<i>0.00212</i>	0.16978
83	Right_LogSpanningForestN_FAMean	0.00067	<i>0.00239</i>	0.18842
234	Left_PGEigengap_FAMean	0.00141	<i>0.00240</i>	0.18684
83	Left_PGEigengap_Unweighted	0.00458	<i>0.00243</i>	0.18738
129	Left_MinCutBalDivSum_FiberLengthMean	0.00892	<i>0.00245</i>	0.18596
83	Left_Sum_FAMean	0.00056	<i>0.00279</i>	0.20893
234	Left_MinCutBalDivSum_Unweighted	0.00154	<i>0.00289</i>	0.21355
234	Left_PGEigengap_FiberLengthMean	0.00554	<i>0.00295</i>	0.21516
234	Right_LogSpanningForestN_FAMean	0.00380	<i>0.00305</i>	0.21935
234	Left_PGEigengap_Unweighted	0.00176	<i>0.00338</i>	0.24029
83	Left_PGEigengap_FAMean	0.00215	<i>0.00359</i>	0.25152
83	Left_LogSpanningForestN_FiberN	0.00012	<i>0.00395</i>	0.27269
129	Left_Sum_Unweighted	0.00232	<i>0.00456</i>	0.31006
83	Left_LogSpanningForestN_FAMean	0.00082	<i>0.00496</i>	0.33212
234	Right_MinCutBalDivSum_Unweighted	0.00462	<i>0.00543</i>	0.35825
83	Right_LogSpanningForestN_FiberNDivLength	0.00022	<i>0.00587</i>	0.38180
234	Left_LogSpanningForestN_FAMean	0.000129	<i>0.00595</i>	0.38054
234	Right_PGEigengap_Unweighted	0.00095	<i>0.00626</i>	0.39459
129	Left_Sum_FAMean	0.00032	<i>0.00660</i>	0.40907
83	Left_AdjLMaxDivD_FiberN	0.00501	<i>0.00804</i>	0.49040
234	Right_Sum_Unweighted	0.00224	<i>0.00845</i>	0.50692
234	Right_PGEigengap_FiberN	0.00009	<i>0.00910</i>	0.53671
129	All_Sum_FiberN	0.00000	<i>0.00938</i>	0.54418

234	Right_PGEigengap_FAMean	0.00074	<i>0.00974</i>	0.55538
129	Right_PGEigengap_FAMean	0.00296	<i>0.00981</i>	0.54933
83	Right_PGEigengap_Unweighted	0.00087	<i>0.01053</i>	0.57889
129	Right_MinCutBalDivSum_FiberN	0.00563	<i>0.01101</i>	0.59432
129	Right_MinCutBalDivSum_Unweighted	0.00492	<i>0.01212</i>	0.64227
129	Left_LogSpanningForestN_FAMean	0.00106	<i>0.01218</i>	0.63359
129	Left_LogSpanningForestN_FiberN	0.00014	<i>0.01258</i>	0.64134
83	All_Sum_FiberN	0.00000	<i>0.01290</i>	0.64480
234	All_Sum_FiberN	0.00000	<i>0.01358</i>	0.66520
83	Right_LogSpanningForestN_Unweighted	0.00541	<i>0.01438</i>	0.69010
129	Left_LogSpanningForestN_FiberNDivLength	0.00288	<i>0.01447</i>	0.67995
129	Right_PGEigengap_Unweighted	0.00242	<i>0.01676</i>	0.77084
129	Right_PGEigengap_FiberN	0.00869	<i>0.01706</i>	0.76750
234	All_MinVertexCover_FAMean	0.00289	<i>0.01713</i>	0.75373
83	All_HoffmanBound_FAMean	0.00087	<i>0.02011</i>	0.86462
83	All_Sum_FiberNDivLength	0.00002	<i>0.02117</i>	0.88929
234	Right_MinCutBalDivSum_FiberN	0.00234	<i>0.02197</i>	0.90065
83	Right_LogSpanningForestN_FiberN	0.00083	<i>0.02539</i>	1.01567
234	Right_MinCutBalDivSum_FiberLengthMean	0.00234	<i>0.02663</i>	1.03841
83	Right_MinCutBalDivSum_FiberNDivLength	0.00072	<i>0.02854</i>	1.08446
129	Left_MinCutBalDivSum_FiberNDivLength	0.00019	<i>0.02897</i>	1.07195
83	Right_PGEigengap_FAMean	0.00112	<i>0.02948</i>	1.06119
234	All_LogSpanningForestN_FiberN	0.00091	<i>0.03308</i>	1.15795
234	Right_PGEigengap_FiberLengthMean	0.00367	<i>0.03369</i>	1.14542
129	Right_MinCutBalDivSum_FiberLengthMean	0.00768	<i>0.04500</i>	1.48511
129	All_Sum_FiberNDivLength	0.00008	<i>0.04728</i>	1.51293
129	Right_LogSpanningForestN_FiberNDivLength	0.00051	<i>0.04891</i>	1.51627
234	All_LogSpanningForestN_FiberNDivLength	0.00106	0.05095	1.52842
129	Right_LogSpanningForestN_FiberN	0.00045	0.05578	1.61751
83	Right_MinCutBalDivSum_FiberN	0.00346	0.06284	1.75951
83	Right_HoffmanBound_FiberNDivLength	0.005129	0.06309	1.70341
83	Right_PGEigengap_FiberLengthMean	0.00949	0.06515	1.69395
234	Left_MinCutBalDivSum_FiberNDivLength	0.00642	0.06548	1.63696
234	Left_MinVertexCover_FAMean	0.00107	0.07139	1.71336
234	All_Sum_FiberNDivLength	0.00044	0.07318	1.68305
83	Right_Sum_FiberN	0.00000	0.07799	1.71586
83	Right_Sum_FiberNDivLength	0.00018	0.07920	1.66329
129	Left_Sum_FiberN	0.00000	0.08380	1.67598
129	Right_Sum_FiberN	0.00001	0.08653	1.64406
129	Left_HoffmanBound_Unweighted	0.00848	0.08944	1.60984
83	Left_Sum_FiberN	0.00000	0.09430	1.60310
234	Left_Sum_FiberN	0.00040	0.11447	1.83157
129	Right_Sum_FiberNDivLength	0.00180	0.12102	1.81523
234	Right_Sum_FiberN	0.00012	0.16411	2.29752
83	Left_Sum_FiberNDivLength	0.00043	0.16774	2.18062
129	Left_Sum_FiberNDivLength	0.00100	0.22542	2.70502
234	Right_Sum_FiberNDivLength	0.00562	0.23691	2.60604
83	Right_HoffmanBound_FAMean	0.00587	0.32069	3.20692
83	All_MinVertexCoverBinary_Unweighted	0.00716	0.38829	3.49459
234	Right_LogSpanningForestN_FiberNDivLength	0.00940	0.40996	3.27971

83	Left_HoffmanBound_FiberN	0.00175	0.41913	2.93394
83	All_MinVertexCover_FiberNDivLength	0.00036	0.46677	2.80065
83	Right_MinSpanningForest_FiberLengthMean	0.00491	0.55239	2.76195
234	Right_MinSpanningForest_FiberLengthMean	0.00601	0.55631	2.22523
129	All_MinVertexCover_FiberN	0.00232	0.71406	2.14217
83	All_MinVertexCover_FiberN	0.00244	0.84437	1.68874
234	All_MinVertexCover_FiberN	0.00055	0.92958	0.92958

Table 1: The results and the statistical analysis of the graph-theoretical evaluation of the sex differences in the 96 diffusion MRI images. The first column gives the resolution in each hemisphere; the number of nodes in the whole graph is 83, 129 and 234, respectively. The second column describes the graph parameter computed: its syntactics is as follows: each parameter-name contains two separating “\_” symbols that define three parts of the parameter-name. The first part describe the hemisphere or the whole connectome with the words Left, Right or All. The second part describes the parameter computed, and the third part the weight function used (their definitions are given in section “Materials and methods”). The third column contains the p-values of the first round, the second column the p-values of the second round, and the third column the (very strict) Holm-Bonferroni correction of the p-value. With  $p=0.05$  *all* the first 12 rows describe significantly different graph theoretical properties between sexes. One-by-one, each row with italic third column describe significant differences between sexes, with  $p=0.05$ . For the details we refer to the section “Statistical analysis”.

## 6. Acknowledgments

The authors declare no conflicts of interest.

## References

- [1] P. Hagmann, P. E. Grant, D. A. Fair, Mr connectomics: a conceptual framework for studying the developing brain., *Front Syst Neurosci* 6 (2012) 43. doi:10.3389/fnsys.2012.00043.  
URL <http://dx.doi.org/10.3389/fnsys.2012.00043>
- [2] R. C. Craddock, M. P. Milham, S. M. LaConte, Predicting intrinsic brain activity., *Neuroimage* 82 (2013) 127–136. doi:10.1016/j.neuroimage.2013.05.072.  
URL <http://dx.doi.org/10.1016/j.neuroimage.2013.05.072>
- [3] G. Ball, P. Aljabar, S. Zebari, N. Tusor, T. Arichi, N. Merchant, E. C. Robinson, E. Ogunjipe, D. Rueckert, A. D. Edwards, S. J. Counsell, Rich-club organization of the newborn human brain., *Proc Natl Acad Sci U S A* 111 (20) (2014) 7456–7461. doi:10.1073/pnas.1324118111.  
URL <http://dx.doi.org/10.1073/pnas.1324118111>

- [4] C. I. Bargmann, Beyond the connectome: how neuromodulators shape neural circuits., *Bioessays* 34 (6) (2012) 458–465. doi:10.1002/bies.201100185.  
URL <http://dx.doi.org/10.1002/bies.201100185>
- [5] D. Batalle, E. Muñoz-Moreno, F. Figueras, N. Bargallo, E. Eixarch, E. Gratacos, Normalization of similarity-based individual brain networks from gray matter MRI and its association with neurodevelopment in infants with intrauterine growth restriction., *Neuroimage* 83 (2013) 901–911. doi:10.1016/j.neuroimage.2013.07.045.  
URL <http://dx.doi.org/10.1016/j.neuroimage.2013.07.045>
- [6] D. J. Graham, Routing in the brain., *Front Comput Neurosci* 8 (2014) 44. doi:10.3389/fncom.2014.00044.  
URL <http://dx.doi.org/10.3389/fncom.2014.00044>
- [7] F. Agosta, S. Galantucci, P. Valsasina, E. Canu, A. Meani, A. Marccone, G. Magnani, A. Falini, G. Comi, M. Filippi, Disrupted brain connectome in semantic variant of primary progressive aphasia., *Neurobiol Aging*doi: 10.1016/j.neurobiolaging.2014.05.017.  
URL <http://dx.doi.org/10.1016/j.neurobiolaging.2014.05.017>
- [8] A. F. Alexander-Bloch, P. T. Reiss, J. Rapoport, H. McAdams, J. N. Giedd, E. T. Bullmore, N. Gogtay, Abnormal cortical growth in schizophrenia targets normative modules of synchronized development., *Biol Psychiatry*doi:10.1016/j.biopsych.2014.02.010.  
URL <http://dx.doi.org/10.1016/j.biopsych.2014.02.010>
- [9] J. T. Baker, A. J. Holmes, G. A. Masters, B. T. T. Yeo, F. Krienen, R. L. Buckner, D. Öngür, Disruption of cortical association networks in schizophrenia and psychotic bipolar disorder., *JAMA Psychiatry* 71 (2) (2014) 109–118. doi:10.1001/jamapsychiatry.2013.3469.  
URL <http://dx.doi.org/10.1001/jamapsychiatry.2013.3469>
- [10] P. Besson, V. Dinkelacker, R. Valabregue, L. Thivard, X. Leclerc, M. Baulac, D. Sammler, O. Colliot, S. Lehericy, S. Samson, S. Dupont, Structural connectivity differences in left and right temporal lobe epilepsy., *Neuroimage* 100C (2014) 135–144. doi:10.1016/j.neuroimage.2014.04.071.  
URL <http://dx.doi.org/10.1016/j.neuroimage.2014.04.071>
- [11] L. Bonilha, T. Nesland, C. Rorden, P. Fillmore, R. P. Ratnayake, J. Fridriksson, Mapping remote subcortical ramifications of injury after ischemic strokes., *Behav Neurol* 2014 (2014) 215380. doi:10.1155/2014/215380.  
URL <http://dx.doi.org/10.1155/2014/215380>

- [12] M. Ingalhalikar, A. Smith, D. Parker, T. D. Satterthwaite, M. A. Elliott, K. Ruparel, H. Hakonarson, R. E. Gur, R. C. Gur, R. Verma, Sex differences in the structural connectome of the human brain., *Proc Natl Acad Sci U S A* 111 (2) (2014) 823–828. doi:10.1073/pnas.1316909110. URL <http://dx.doi.org/10.1073/pnas.1316909110>
- [13] D. Joel, R. Tarrasch, On the mis-presentation and misinterpretation of gender-related data: the case of Ingalhalikar’s human connectome study., *Proc Natl Acad Sci U S A* 111 (6) (2014) E637. doi:10.1073/pnas.1323319111. URL <http://dx.doi.org/10.1073/pnas.1323319111>
- [14] M. Ingalhalikar, A. Smith, D. Parker, T. D. Satterthwaite, M. A. Elliott, K. Ruparel, H. Hakonarson, R. E. Gur, R. C. Gur, R. Verma, Reply to Joel and Tarrasch: On misreading and shooting the messenger., *Proc Natl Acad Sci U S A* 111 (6) (2014) E638.
- [15] C. Fine, Neuroscience. his brain, her brain?, *Science* 346 (6212) (2014) 915–916. doi:10.1126/science.1262061. URL <http://dx.doi.org/10.1126/science.1262061>
- [16] S. F. Witelson, H. Beresh, D. L. Kigar, Intelligence and brain size in 100 postmortem brains: sex, lateralization and age factors., *Brain* 129 (Pt 2) (2006) 386–398. doi:10.1093/brain/awh696. URL <http://dx.doi.org/10.1093/brain/awh696>
- [17] Y. Taki, B. Thyreau, S. Kinomura, K. Sato, R. Goto, R. Kawashima, H. Fukuda, Correlations among brain gray matter volumes, age, gender, and hemisphere in healthy individuals., *PLoS One* 6 (7) (2011) e22734. doi:10.1371/journal.pone.0022734. URL <http://dx.doi.org/10.1371/journal.pone.0022734>
- [18] E. L. Lawler, *Combinatorial optimization: networks and matroids*, Courier Dover Publications, 1976.
- [19] L. R. Ford, D. R. Fulkerson, Maximal flow through a network, *Canadian Journal of Mathematics* 8 (3) (1956) 399–404.
- [20] P. Ade, N. Aghanim, C. Armitage-Caplan, M. Arnaud, M. Ashdown, F. Atrio-Barandela, J. Aumont, C. Baccigalupi, A. Banday, R. Barreiro, et al., Planck 2013 results. XVI. Cosmological parameters, arXiv preprint arXiv:1303.5076.
- [21] M. R. Garey, D. S. Johnson, L. Stockmeyer, Some simplified NP-complete graph problems, *Theoretical computer science* 1 (3) (1976) 237–267.
- [22] R. E. Tarjan, *Data structures and network algorithms*, Vol. 44 of CBMS-NSF Regional Conference Series in Applied Mathematics, Society for Industrial Applied Mathematics, 1983.

- [23] S. Hoory, N. Linial, A. Wigderson, Expander graphs and their applications, *Bulletin of the American Mathematical Society* 43 (4) (2006) 439–561.
- [24] L. Lovász, *Combinatorial problems and exercises*, 2nd Edition, American Mathematical Society, 2007.
- [25] H. Prüfer, Neuer Beweis eines Satzes über Permutationen, *Arch. Math. Phys* 27 (1918) 742–744.
- [26] G. Kirchhoff, über die Auflösung der Gleichungen, auf welche man bei der untersuchung der linearen verteilung galvanischer Ströme geführt wird, *Ann. Phys. Chem.* 72.
- [27] F. R. Chung, *Spectral graph theory*, Vol. 92, American Mathematical Soc., 1997.
- [28] J. A. McNab, B. L. Edlow, T. Witzel, S. Y. Huang, H. Bhat, K. Heberlein, T. Feiweier, K. Liu, B. Keil, J. Cohen-Adad, M. D. Tisdall, R. D. Folkert, H. C. Kinney, L. L. Wald, The Human Connectome Project and beyond: initial applications of 300 mT/m gradients., *Neuroimage* 80 (2013) 234–245. doi:10.1016/j.neuroimage.2013.05.074. URL <http://dx.doi.org/10.1016/j.neuroimage.2013.05.074>
- [29] A. Daducci, S. Gerhard, A. Griffa, A. Lemkaddem, L. Cammoun, X. Giggandet, R. Meuli, P. Hagmann, J.-P. Thiran, The connectome mapper: an open-source processing pipeline to map connectomes with MRI., *PLoS One* 7 (12) (2012) e48121. doi:10.1371/journal.pone.0048121. URL <http://dx.doi.org/10.1371/journal.pone.0048121>
- [30] P. J. Basser, C. Pierpaoli, Microstructural and physiological features of tissues elucidated by quantitative-diffusion-tensor mri. 1996., *J Magn Reson* 213 (2) (2011) 560–570. doi:10.1016/j.jmr.2011.09.022. URL <http://dx.doi.org/10.1016/j.jmr.2011.09.022>
- [31] D. S. Hochbaum, Approximation algorithms for the set covering and vertex cover problems, *SIAM Journal on Computing* 11 (3) (1982) 555–556.
- [32] T. Achterberg, T. Berthold, T. Koch, K. Wolter, Constraint integer programming: A new approach to integrate CP and MIP, in: *Integration of AI and OR techniques in constraint programming for combinatorial optimization problems*, Springer, 2008, pp. 6–20.
- [33] T. Achterberg, Scip: solving constraint integer programs, *Mathematical Programming Computation* 1 (1) (2009) 1–41.
- [34] P. G. Hoel, *Introduction to mathematical statistics.*, 5th Edition, John Wiley & Sons, Inc., New York, 1984.
- [35] T. H. Wonnacott, R. J. Wonnacott, *Introductory statistics*, Vol. 19690, Wiley New York, 1972.



- [36] S. Holm, A simple sequentially rejective multiple test procedure, *Scandinavian Journal of Statistics* (1979) 65–70.

## Appendix

In this appendix we list the graph-theoretic parameters computed for the resolutions of 83, 129 and 234 vertex graphs. The tables contain their arithmetic means in the male and female groups, and the corresponding p-values. The values in these tables contain the values corresponded to round 1 (see the “Statistical analysis” subsection in the main text).

The graph-parameters are defined in the caption of Table 1.

Significant differences ( $p < 0.01$ ) are denoted with an asterisk in the last column.

### Scale 83, round 1

Property	Female	Male	p-value
All_AdjLMaxDivD_FAMean	1.36008	1.37750	0.06806
All_AdjLMaxDivD_FiberLengthMean	1.44214	1.43602	0.72030
All_AdjLMaxDivD_FiberN	2.02416	2.10529	0.05606
All_AdjLMaxDivD_FiberNDivLength	1.84476	1.86864	0.41834
All_AdjLMaxDivD_Unweighted	1.26760	1.26456	0.63251
All_HoffmanBound_FAMean	4.36096	4.18564	0.00087 *
All_HoffmanBound_FiberLengthMean	3.21938	3.26552	0.33136
All_HoffmanBound_FiberN	2.63525	2.55573	0.03144
All_HoffmanBound_FiberNDivLength	2.51038	2.40550	0.01815
All_HoffmanBound_Unweighted	4.55192	4.43931	0.04616
All_LogSpanningForestN_FAMean	110.69890	101.82758	0.00012 *
All_LogSpanningForestN_FiberLengthMean	456.60084	452.95875	0.18687
All_LogSpanningForestN_FiberN	397.53780	389.79037	0.00001 *
All_LogSpanningForestN_FiberNDivLength	148.03174	139.85355	0.00003 *
All_LogSpanningForestN_Unweighted	191.66035	187.85180	0.00113 *
All_MinCutBalDivSum_FAMean	0.00793	0.00474	0.14869
All_MinCutBalDivSum_FiberLengthMean	0.03115	0.02889	0.47008
All_MinCutBalDivSum_FiberN	0.02924	0.02711	0.34092
All_MinCutBalDivSum_FiberNDivLength	0.02868	0.02644	0.38768
All_MinCutBalDivSum_Unweighted	0.04001	0.03721	0.28887
All_MinSpanningForest_FAMean	19.78188	18.63722	0.02232
All_MinSpanningForest_FiberLengthMean	1096.37958	1112.97289	0.10506
All_MinSpanningForest_FiberN	99.53846	102.93333	0.14280
All_MinSpanningForest_FiberNDivLength	3.65548	3.66822	0.93669
All_MinVertexCoverBinary_Unweighted	59.80769	59.00000	0.00716 *
All_MinVertexCover_FAMean	18.73144	18.10619	0.01699
All_MinVertexCover_FiberLengthMean	2014.06431	1955.70824	0.37460
All_MinVertexCover_FiberN	2427.21154	2315.20000	0.00244 *
All_MinVertexCover_FiberNDivLength	110.25657	103.59777	0.00036 *
All_MinVertexCover_Unweighted	40.90385	41.00000	0.32897
All_PGEigengap_FAMean	0.05403	0.05071	0.28914
All_PGEigengap_FiberLengthMean	0.04167	0.03891	0.43309
All_PGEigengap_FiberN	0.03156	0.02829	0.03885
All_PGEigengap_FiberNDivLength	0.03470	0.03062	0.01847
All_PGEigengap_Unweighted	0.05214	0.04740	0.09708
All_Sum_FAMean	222.01291	201.02562	0.00029 *
All_Sum_FiberLengthMean	16845.33062	15792.24352	0.06219
All_Sum_FiberN	11261.65385	10237.13333	0.00000 *
All_Sum_FiberNDivLength	476.56342	433.37987	0.00002 *
All_Sum_Unweighted	567.07692	539.80000	0.00025 *
Left_AdjLMaxDivD_FAMean	1.33644	1.35216	0.15767
Left_AdjLMaxDivD_FiberLengthMean	1.40515	1.38890	0.32795
Left_AdjLMaxDivD_FiberN	1.90607	2.02087	0.00501 *
Left_AdjLMaxDivD_FiberNDivLength	1.71498	1.77482	0.07539
Left_AdjLMaxDivD_Unweighted	1.24027	1.23523	0.43598
Left_HoffmanBound_FAMean	4.55406	4.38621	0.01297
Left_HoffmanBound_FiberLengthMean	3.25098	3.28435	0.51250
Left_HoffmanBound_FiberN	2.71430	2.61098	0.00175 *

Left_HoffmanBound_FiberNDivLength	2.66652	2.59451	0.13782	
Left_HoffmanBound_Unweighted	4.73205	4.57434	0.01379	
Left_LogSpanningForestN_FAMean	53.30579	48.82905	0.00082	*
Left_LogSpanningForestN_FiberLengthMean	229.63370	227.32675	0.18765	
Left_LogSpanningForestN_FiberN	199.27958	195.25428	0.00012	*
Left_LogSpanningForestN_FiberNDivLength	73.53683	69.82889	0.00343	*
Left_LogSpanningForestN_Unweighted	95.46307	93.39767	0.01389	
Left_MinCutBalDivSum_FAMean	0.00687	0.00320	0.17151	
Left_MinCutBalDivSum_FiberLengthMean	0.23438	0.21147	0.01779	
Left_MinCutBalDivSum_FiberN	0.13337	0.12011	0.00403	*
Left_MinCutBalDivSum_FiberNDivLength	0.11057	0.09321	0.00031	*
Left_MinCutBalDivSum_Unweighted	0.24513	0.22019	0.00206	*
Left_MinSpanningForest_FAMean	9.57924	9.06313	0.04242	
Left_MinSpanningForest_FiberLengthMean	561.47024	560.36391	0.87722	
Left_MinSpanningForest_FiberN	51.23077	53.73333	0.26795	
Left_MinSpanningForest_FiberNDivLength	1.82447	1.89521	0.62729	
Left_MinVertexCoverBinary_Unweighted	30.23077	29.73333	0.09601	
Left_MinVertexCover_FAMean	9.23616	8.88642	0.01371	
Left_MinVertexCover_FiberLengthMean	1064.27185	1027.73430	0.35926	
Left_MinVertexCover_FiberN	1158.21154	1143.46667	0.55321	
Left_MinVertexCover_FiberNDivLength	54.26322	51.17634	0.02122	
Left_MinVertexCover_Unweighted	20.80769	20.83333	0.75017	
Left_PGEigengap_FAMean	0.33446	0.29469	0.00215	*
Left_PGEigengap_FiberLengthMean	0.33383	0.29287	0.01329	
Left_PGEigengap_FiberN	0.16980	0.15238	0.01654	
Left_PGEigengap_FiberNDivLength	0.14486	0.13413	0.02837	
Left_PGEigengap_Unweighted	0.30646	0.27160	0.00458	*
Left_Sum_FAMean	106.64056	96.80731	0.00056	*
Left_Sum_FiberLengthMean	8629.73791	8122.82646	0.13250	
Left_Sum_FiberN	5514.61538	5049.73333	0.00000	*
Left_Sum_FiberNDivLength	233.06402	213.49323	0.00043	*
Left_Sum_Unweighted	282.50000	269.06667	0.00378	*
Right_AdjLMaxDivD_FAMean	1.32878	1.34242	0.14511	
Right_AdjLMaxDivD_FiberLengthMean	1.39672	1.38478	0.30191	
Right_AdjLMaxDivD_FiberN	2.00803	2.09048	0.05380	
Right_AdjLMaxDivD_FiberNDivLength	1.76990	1.81343	0.09784	
Right_AdjLMaxDivD_Unweighted	1.25268	1.24720	0.29540	
Right_HoffmanBound_FAMean	4.47438	4.28666	0.00587	*
Right_HoffmanBound_FiberLengthMean	3.33823	3.39478	0.29902	
Right_HoffmanBound_FiberN	2.67311	2.57701	0.05411	
Right_HoffmanBound_FiberNDivLength	2.62635	2.48983	0.00560	*
Right_HoffmanBound_Unweighted	4.61480	4.50726	0.03806	
Right_LogSpanningForestN_FAMean	52.25642	48.14346	0.00067	*
Right_LogSpanningForestN_FiberLengthMean	218.25106	216.24411	0.16431	
Right_LogSpanningForestN_FiberN	190.62427	187.02757	0.00083	*
Right_LogSpanningForestN_FiberNDivLength	69.84080	66.17446	0.00022	*
Right_LogSpanningForestN_Unweighted	90.24090	88.51678	0.00541	*
Right_MinCutBalDivSum_FAMean	0.02476	0.00851	0.00496	*
Right_MinCutBalDivSum_FiberLengthMean	0.24577	0.22309	0.02216	
Right_MinCutBalDivSum_FiberN	0.13346	0.12050	0.00346	*
Right_MinCutBalDivSum_FiberNDivLength	0.10831	0.09357	0.00072	*
Right_MinCutBalDivSum_Unweighted	0.23713	0.22022	0.01629	
Right_MinSpanningForest_FAMean	10.30911	9.79708	0.10419	
Right_MinSpanningForest_FiberLengthMean	532.13580	547.85331	0.00491	*
Right_MinSpanningForest_FiberN	50.76923	52.53333	0.26282	
Right_MinSpanningForest_FiberNDivLength	1.94340	1.89232	0.58863	
Right_MinVertexCoverBinary_Unweighted	29.07692	28.73333	0.15457	
Right_MinVertexCover_FAMean	9.26572	9.03965	0.12382	
Right_MinVertexCover_FiberLengthMean	934.26071	897.95882	0.23661	
Right_MinVertexCover_FiberN	1169.63462	1122.93333	0.07986	
Right_MinVertexCover_FiberNDivLength	53.57144	51.50298	0.10452	
Right_MinVertexCover_Unweighted	20.11538	20.26667	0.10527	
Right_PGEigengap_FAMean	0.32454	0.28808	0.00112	*
Right_PGEigengap_FiberLengthMean	0.34029	0.29461	0.00949	*
Right_PGEigengap_FiberN	0.17666	0.15912	0.02617	
Right_PGEigengap_FiberNDivLength	0.15245	0.14034	0.01613	
Right_PGEigengap_Unweighted	0.29582	0.26081	0.00087	*
Right_Sum_FAMean	105.62164	95.26436	0.00028	*

Right_Sum_FiberLengthMean	7644.90330	7086.91000	0.02974	
Right_Sum_FiberN	5378.03846	4884.66667	0.00000	*
Right_Sum_FiberNDivLength	225.94776	206.97587	0.00018	*
Right_Sum_Unweighted	261.30769	248.26667	0.00019	*

Scale 129, round 1

Property	Female	Male	p-value	
All_AdjLMaxDivD_FAMean	1.40519	1.42604	0.10040	
All_AdjLMaxDivD_FiberLengthMean	1.50483	1.50158	0.87806	
All_AdjLMaxDivD_FiberN	2.14552	2.22254	0.15242	
All_AdjLMaxDivD_FiberNDivLength	2.09783	2.04782	0.32031	
All_AdjLMaxDivD_Unweighted	1.30028	1.29097	0.27278	
All_HoffmanBound_FAMean	4.40157	4.29660	0.02644	
All_HoffmanBound_FiberLengthMean	3.19684	3.24689	0.32568	
All_HoffmanBound_FiberN	2.50604	2.48884	0.64956	
All_HoffmanBound_FiberNDivLength	2.34647	2.41938	0.07720	
All_HoffmanBound_Unweighted	4.62935	4.51267	0.01233	
All_LogSpanningForestN_FAMean	194.37749	181.03525	0.00019	*
All_LogSpanningForestN_FiberLengthMean	739.78985	732.55388	0.09867	
All_LogSpanningForestN_FiberN	599.76631	588.61699	0.00000	*
All_LogSpanningForestN_FiberNDivLength	210.52236	200.75240	0.00000	*
All_LogSpanningForestN_Unweighted	322.09324	316.62672	0.00218	*
All_MinCutBalDivSum_FAMean	0.00668	0.00324	0.05930	
All_MinCutBalDivSum_FiberLengthMean	0.01706	0.01607	0.56293	
All_MinCutBalDivSum_FiberN	0.02658	0.02429	0.26627	
All_MinCutBalDivSum_FiberNDivLength	0.02495	0.02258	0.30029	
All_MinCutBalDivSum_Unweighted	0.02218	0.02065	0.30082	
All_MinSpanningForest_FAMean	30.14746	28.58509	0.02073	
All_MinSpanningForest_FiberLengthMean	1642.68263	1664.23693	0.07510	
All_MinSpanningForest_FiberN	140.23077	140.93333	0.55077	
All_MinSpanningForest_FiberNDivLength	4.42401	4.43795	0.92181	
All_MinVertexCoverBinary_Unweighted	96.46154	96.26667	0.66793	
All_MinVertexCover_FAMean	29.56250	28.72424	0.02181	
All_MinVertexCover_FiberLengthMean	3230.07900	3121.21684	0.29100	
All_MinVertexCover_FiberN	2444.92308	2337.40000	0.00232	*
All_MinVertexCover_FiberNDivLength	120.18766	116.22553	0.02502	
All_MinVertexCover_Unweighted	63.88462	63.96667	0.35805	
All_PGEigengap_FAMean	0.03143	0.02928	0.25524	
All_PGEigengap_FiberLengthMean	0.02427	0.02260	0.43054	
All_PGEigengap_FiberN	0.02781	0.02453	0.01902	
All_PGEigengap_FiberNDivLength	0.02880	0.02498	0.00792	*
All_PGEigengap_Unweighted	0.03012	0.02725	0.09661	
All_Sum_FAMean	397.68878	360.50850	0.00015	*
All_Sum_FiberLengthMean	30670.09535	28478.19852	0.03582	
All_Sum_FiberN	12375.61538	11458.13333	0.00000	*
All_Sum_FiberNDivLength	548.61301	510.71378	0.00008	*
All_Sum_Unweighted	1020.80769	972.86667	0.00026	*
Left_AdjLMaxDivD_FAMean	1.37823	1.39812	0.12792	
Left_AdjLMaxDivD_FiberLengthMean	1.43638	1.42179	0.36739	
Left_AdjLMaxDivD_FiberN	1.84672	1.92762	0.12247	
Left_AdjLMaxDivD_FiberNDivLength	1.77313	1.80979	0.33521	
Left_AdjLMaxDivD_Unweighted	1.26380	1.25501	0.16858	
Left_HoffmanBound_FAMean	4.57539	4.44885	0.01512	
Left_HoffmanBound_FiberLengthMean	3.23550	3.25088	0.77158	
Left_HoffmanBound_FiberN	2.80373	2.74220	0.14090	
Left_HoffmanBound_FiberNDivLength	2.70077	2.64308	0.21782	
Left_HoffmanBound_Unweighted	4.75280	4.61941	0.00848	*
Left_LogSpanningForestN_FAMean	96.11000	89.25516	0.00106	*
Left_LogSpanningForestN_FiberLengthMean	373.09476	368.65582	0.08843	
Left_LogSpanningForestN_FiberN	300.77613	295.83044	0.00014	*
Left_LogSpanningForestN_FiberNDivLength	105.01323	100.80980	0.00288	*
Left_LogSpanningForestN_Unweighted	162.01302	158.88026	0.01336	
Left_MinCutBalDivSum_FAMean	0.00873	0.00273	0.05683	
Left_MinCutBalDivSum_FiberLengthMean	0.19822	0.17378	0.00892	*
Left_MinCutBalDivSum_FiberN	0.12848	0.10467	0.00001	*
Left_MinCutBalDivSum_FiberNDivLength	0.06926	0.05546	0.00019	*

Left_MinCutBalDivSum_Unweighted	0.19535	0.17339	0.00265	*
Left_MinSpanningForest_FAMean	14.57467	13.88500	0.06189	
Left_MinSpanningForest_FiberLengthMean	828.34729	834.54850	0.36946	
Left_MinSpanningForest_FiberN	69.30769	72.20000	0.02902	
Left_MinSpanningForest_FiberNDivLength	2.16989	2.25626	0.53695	
Left_MinVertexCoverBinary_Unweighted	48.76923	48.86667	0.69355	
Left_MinVertexCover_FAMean	14.65360	14.09857	0.01273	
Left_MinVertexCover_FiberLengthMean	1700.29684	1637.18742	0.30481	
Left_MinVertexCover_FiberN	1169.82692	1125.20000	0.06266	
Left_MinVertexCover_FiberNDivLength	58.76113	56.23736	0.06303	
Left_MinVertexCover_Unweighted	32.28846	32.30000	0.88865	
Left_PGEigengap_FAMean	0.22611	0.19656	0.00995	*
Left_PGEigengap_FiberLengthMean	0.23241	0.20065	0.02197	
Left_PGEigengap_FiberN	0.12346	0.10569	0.00382	*
Left_PGEigengap_FiberNDivLength	0.09689	0.08572	0.00223	*
Left_PGEigengap_Unweighted	0.20204	0.17516	0.01081	
Left_Sum_FAMean	197.41850	178.80563	0.00032	*
Left_Sum_FiberLengthMean	16079.40944	14931.40760	0.07487	
Left_Sum_FiberN	6071.96154	5641.93333	0.00000	*
Left_Sum_FiberNDivLength	269.09760	251.40080	0.00100	*
Left_Sum_Unweighted	519.53846	492.86667	0.00232	*
Right_AdjLMaxDivD_FAMean	1.35746	1.36837	0.36353	
Right_AdjLMaxDivD_FiberLengthMean	1.42015	1.41129	0.54264	
Right_AdjLMaxDivD_FiberN	2.05564	2.19134	0.01338	
Right_AdjLMaxDivD_FiberNDivLength	1.82146	1.86716	0.20816	
Right_AdjLMaxDivD_Unweighted	1.26684	1.25522	0.12057	
Right_HoffmanBound_FAMean	4.37886	4.29574	0.20294	
Right_HoffmanBound_FiberLengthMean	3.32686	3.36662	0.49418	
Right_HoffmanBound_FiberN	2.66511	2.56838	0.01727	
Right_HoffmanBound_FiberNDivLength	2.68679	2.59830	0.01992	
Right_HoffmanBound_Unweighted	4.60861	4.51407	0.08448	
Right_LogSpanningForestN_FAMean	93.41904	87.28295	0.00143	*
Right_LogSpanningForestN_FiberLengthMean	358.00491	354.73456	0.14280	
Right_LogSpanningForestN_FiberN	291.08563	285.72242	0.00045	*
Right_LogSpanningForestN_FiberNDivLength	100.74383	96.22891	0.00051	*
Right_LogSpanningForestN_Unweighted	154.36558	151.96595	0.01158	
Right_MinCutBalDivSum_FAMean	0.02361	0.01005	0.00807	*
Right_MinCutBalDivSum_FiberLengthMean	0.20000	0.17303	0.00768	*
Right_MinCutBalDivSum_FiberN	0.11452	0.10111	0.00563	*
Right_MinCutBalDivSum_FiberNDivLength	0.06865	0.06326	0.09375	
Right_MinCutBalDivSum_Unweighted	0.19180	0.16911	0.00492	*
Right_MinSpanningForest_FAMean	15.61479	14.88977	0.06537	
Right_MinSpanningForest_FiberLengthMean	808.14079	824.37649	0.03729	
Right_MinSpanningForest_FiberN	70.46154	68.93333	0.07096	
Right_MinSpanningForest_FiberNDivLength	2.32813	2.26810	0.46298	
Right_MinVertexCoverBinary_Unweighted	47.34615	47.00000	0.29760	
Right_MinVertexCover_FAMean	14.70648	14.40974	0.13709	
Right_MinVertexCover_FiberLengthMean	1516.99670	1461.52391	0.23679	
Right_MinVertexCover_FiberN	1175.50000	1166.36667	0.68666	
Right_MinVertexCover_FiberNDivLength	59.59421	58.78162	0.47843	
Right_MinVertexCover_Unweighted	31.61538	31.73333	0.20363	
Right_PGEigengap_FAMean	0.22838	0.19627	0.00296	*
Right_PGEigengap_FiberLengthMean	0.23840	0.19868	0.01013	
Right_PGEigengap_FiberN	0.12500	0.11049	0.00869	*
Right_PGEigengap_FiberNDivLength	0.10075	0.09371	0.03033	
Right_PGEigengap_Unweighted	0.20584	0.17429	0.00242	*
Right_Sum_FAMean	190.48228	172.48988	0.00062	*
Right_Sum_FiberLengthMean	13952.01182	13003.32443	0.04620	
Right_Sum_FiberN	5935.73077	5525.26667	0.00001	*
Right_Sum_FiberNDivLength	262.31420	246.32048	0.00180	*
Right_Sum_Unweighted	477.38462	454.86667	0.00068	*

Scale 234, round 1

Property	Female	Male	p-value
All_AdjLMaxDivD_FAMean	2.15050	2.14489	0.86385
All_AdjLMaxDivD_FiberLengthMean	2.35868	2.34695	0.80876

All_AdjLMaxDivD_FiberN	5.14838	5.00652	0.35870
All_AdjLMaxDivD_FiberNDivLength	5.17072	4.78287	0.02543
All_AdjLMaxDivD_Unweighted	1.89062	1.84578	0.06482
All_HoffmanBound_FAMean	3.63940	3.62013	0.57408
All_HoffmanBound_FiberLengthMean	2.92490	2.98466	0.17340
All_HoffmanBound_FiberN	2.23619	2.26557	0.30055
All_HoffmanBound_FiberNDivLength	2.20178	2.23871	0.13550
All_HoffmanBound_Unweighted	3.73661	3.72935	0.82472
All_LogSpanningForestN_FAMean	446.86116	416.54482	0.03232
All_LogSpanningForestN_FiberLengthMean	2324.68381	2325.52712	0.96824
All_LogSpanningForestN_FiberN	1456.24015	1445.53700	0.36683
All_LogSpanningForestN_FiberNDivLength	149.01647	138.16817	0.15229
All_LogSpanningForestN_Unweighted	942.01654	944.27877	0.83734
All_MinCutBalDivSum_FAMean	0.00000	0.00000	nan
All_MinCutBalDivSum_FiberLengthMean	0.00769	0.00723	0.57442
All_MinCutBalDivSum_FiberN	0.02405	0.02168	0.21132
All_MinCutBalDivSum_FiberNDivLength	0.00000	0.00000	0.45008
All_MinCutBalDivSum_Unweighted	0.00898	0.00834	0.32475
All_MinSpanningForest_FAMean	98.19730	92.47667	0.00151
All_MinSpanningForest_FiberLengthMean	5358.83904	5379.38212	0.44199
All_MinSpanningForest_FiberN	481.46154	479.20000	0.45787
All_MinSpanningForest_FiberNDivLength	18.53246	18.36575	0.71037
All_MinVertexCoverBinary_Unweighted	276.15385	280.33333	0.12225
All_MinVertexCover_FAMean	89.53747	87.25805	0.06974
All_MinVertexCover_FiberLengthMean	8136.04292	7957.20990	0.48358
All_MinVertexCover_FiberN	2430.61538	2344.50000	0.00056
All_MinVertexCover_FiberNDivLength	129.82332	126.64639	0.02087
All_MinVertexCover_Unweighted	222.57692	223.33333	0.39844
All_PGEigengap_FAMean	0.01106	0.01201	0.54543
All_PGEigengap_FiberLengthMean	0.00860	0.00960	0.45409
All_PGEigengap_FiberN	0.01894	0.01927	0.89543
All_PGEigengap_FiberNDivLength	0.01773	0.01767	0.97772
All_PGEigengap_Unweighted	0.00995	0.01067	0.59117
All_Sum_FAMean	1033.36931	961.08503	0.00297
All_Sum_FiberLengthMean	74747.99556	71461.78993	0.18467
All_Sum_FiberN	13609.34615	12823.40000	0.00000
All_Sum_FiberNDivLength	652.17760	623.38731	0.00139
All_Sum_Unweighted	2801.69231	2746.20000	0.21290
Left_AdjLMaxDivD_FAMean	2.14627	2.14335	0.93401
Left_AdjLMaxDivD_FiberLengthMean	2.29338	2.29214	0.97718
Left_AdjLMaxDivD_FiberN	4.03186	4.16381	0.29128
Left_AdjLMaxDivD_FiberNDivLength	3.93717	3.84897	0.38654
Left_AdjLMaxDivD_Unweighted	1.86339	1.81508	0.04174
Left_HoffmanBound_FAMean	3.74670	3.77335	0.55549
Left_HoffmanBound_FiberLengthMean	2.94312	2.99233	0.25660
Left_HoffmanBound_FiberN	2.51168	2.47461	0.28318
Left_HoffmanBound_FiberNDivLength	2.44470	2.45140	0.85286
Left_HoffmanBound_Unweighted	3.82814	3.84621	0.65499
Left_LogSpanningForestN_FAMean	212.18613	197.08273	0.04326
Left_LogSpanningForestN_FiberLengthMean	1159.44274	1165.33847	0.58696
Left_LogSpanningForestN_FiberN	723.10349	723.01322	0.98899
Left_LogSpanningForestN_FiberNDivLength	70.44766	65.77187	0.31060
Left_LogSpanningForestN_Unweighted	467.24325	470.94213	0.52729
Left_MinCutBalDivSum_FAMean	0.00000	0.00000	nan
Left_MinCutBalDivSum_FiberLengthMean	0.09355	0.07667	0.00655
Left_MinCutBalDivSum_FiberN	0.07158	0.05914	0.00062
Left_MinCutBalDivSum_FiberNDivLength	0.00000	0.00000	nan
Left_MinCutBalDivSum_Unweighted	0.09416	0.07896	0.00153
Left_MinSpanningForest_FAMean	47.28302	44.78250	0.00239
Left_MinSpanningForest_FiberLengthMean	2702.23206	2712.65026	0.49327
Left_MinSpanningForest_FiberN	244.11538	244.46667	0.89014
Left_MinSpanningForest_FiberNDivLength	9.45842	9.50259	0.88229
Left_MinVertexCoverBinary_Unweighted	137.19231	140.00000	0.06105
Left_MinVertexCover_FAMean	43.50481	42.59720	0.16942
Left_MinVertexCover_FiberLengthMean	4136.87086	4052.71473	0.55895
Left_MinVertexCover_FiberN	1168.19231	1153.66667	0.46021
Left_MinVertexCover_FiberNDivLength	63.94002	64.04107	0.92511
Left_MinVertexCover_Unweighted	111.38462	112.26667	0.09259

Left_PGEigengap_FAMean	0.08402	0.07554	0.28777
Left_PGEigengap_FiberLengthMean	0.08669	0.07722	0.29463
Left_PGEigengap_FiberN	0.06812	0.05737	0.09675
Left_PGEigengap_FiberNDivLength	0.05084	0.04481	0.18106
Left_PGEigengap_Unweighted	0.07190	0.06398	0.24844
Left_Sum_FAMean	504.02280	470.30921	0.01077
Left_Sum_FiberLengthMean	38178.70022	36255.83071	0.19037
Left_Sum_FiberN	6716.53846	6389.20000	0.00107 *
Left_Sum_FiberNDivLength	322.55630	311.23280	0.04079
Left_Sum_Unweighted	1401.80769	1380.33333	0.39428
Right_AdjLMaxDivD_FAMean	2.00996	2.02718	0.61502
Right_AdjLMaxDivD_FiberLengthMean	2.15381	2.18170	0.41400
Right_AdjLMaxDivD_FiberN	4.11898	4.41926	0.03397
Right_AdjLMaxDivD_FiberNDivLength	3.79534	3.75488	0.70781
Right_AdjLMaxDivD_Unweighted	1.79189	1.77141	0.38704
Right_HoffmanBound_FAMean	3.63008	3.59884	0.45778
Right_HoffmanBound_FiberLengthMean	3.00591	3.02300	0.69490
Right_HoffmanBound_FiberN	2.40837	2.33314	0.00150 *
Right_HoffmanBound_FiberNDivLength	2.45857	2.38848	0.01602
Right_HoffmanBound_Unweighted	3.71704	3.69299	0.50645
Right_LogSpanningForestN_FAMean	228.90719	215.28259	0.07936
Right_LogSpanningForestN_FiberLengthMean	1154.04516	1148.91122	0.63377
Right_LogSpanningForestN_FiberN	724.05083	716.03208	0.22608
Right_LogSpanningForestN_FiberNDivLength	72.92465	68.45678	0.30478
Right_LogSpanningForestN_Unweighted	467.61765	466.56728	0.85195
Right_MinCutBalDivSum_FAMean	0.00050	0.00000	0.19303
Right_MinCutBalDivSum_FiberLengthMean	0.10021	0.08439	0.01271
Right_MinCutBalDivSum_FiberN	0.07599	0.06701	0.00641 *
Right_MinCutBalDivSum_FiberNDivLength	0.00034	0.00000	0.18042
Right_MinCutBalDivSum_Unweighted	0.09573	0.08171	0.01034
Right_MinSpanningForest_FAMean	50.98056	47.79220	0.00435 *
Right_MinSpanningForest_FiberLengthMean	2655.83115	2655.71544	0.99483
Right_MinSpanningForest_FiberN	238.96154	236.00000	0.15420
Right_MinSpanningForest_FiberNDivLength	9.28191	9.00082	0.18645
Right_MinVertexCoverBinary_Unweighted	138.30769	140.00000	0.25603
Right_MinVertexCover_FAMean	45.80119	44.57707	0.07765
Right_MinVertexCover_FiberLengthMean	3994.00115	3884.90036	0.36802
Right_MinVertexCover_FiberN	1144.80769	1129.73333	0.41752
Right_MinVertexCover_FiberNDivLength	62.35579	61.50301	0.47854
Right_MinVertexCover_Unweighted	111.09615	111.10000	0.99385
Right_PGEigengap_FAMean	0.08312	0.07683	0.33378
Right_PGEigengap_FiberLengthMean	0.08538	0.07887	0.40909
Right_PGEigengap_FiberN	0.06631	0.06080	0.28067
Right_PGEigengap_FiberNDivLength	0.05084	0.04854	0.52890
Right_PGEigengap_Unweighted	0.07102	0.06430	0.25554
Right_Sum_FAMean	517.36095	481.68012	0.00745 *
Right_Sum_FiberLengthMean	35857.03890	34486.76733	0.26347
Right_Sum_FiberN	6524.53846	6187.46667	0.00050 *
Right_Sum_FiberNDivLength	312.50248	299.09835	0.01170
Right_Sum_Unweighted	1368.00000	1339.06667	0.20464